

RGS12 and RGS14 GoLoco Motifs Are $G\alpha_i$ Interaction Sites with Guanine Nucleotide Dissociation Inhibitor Activity*

Received for publication, April 11, 2001, and in revised form, May 14, 2001
Published, JBC Papers in Press, May 31, 2001, DOI 10.1074/jbc.M103208200

Randall J. Kimple[‡], Luc De Vries[§], Hélène Tronchère[¶], Cynthia I. Behe, Rebecca A. Morris, Marilyn Gist Farquhar[§], and David P. Siderovski^{||}

From the Department of Pharmacology, Lineberger Comprehensive Cancer Center, and University of North Carolina Neuroscience Center, University of North Carolina, Chapel Hill, North Carolina 27599-7365, the [§]Department of Cellular and Molecular Medicine, University of California at San Diego, La Jolla, CA 92093-0651, and [¶]INSERM U326, 31059 Toulouse Cedex 3, France

The regulators of G-protein signaling (RGS) proteins accelerate the intrinsic guanosine triphosphatase activity of heterotrimeric G-protein α subunits and are thus recognized as key modulators of G-protein-coupled receptor signaling. RGS12 and RGS14 contain not only the hallmark RGS box responsible for GTPase-accelerating activity but also a single $G\alpha_{i/o}$ -Loco (GoLoco) motif predicted to represent a second $G\alpha$ interaction site. Here, we describe functional characterization of the GoLoco motif regions of RGS12 and RGS14. Both regions interact exclusively with $G\alpha_{i1}$, $G\alpha_{i2}$, and $G\alpha_{i3}$ in their GDP-bound forms. In GTP γ S binding assays, both regions exhibit guanine nucleotide dissociation inhibitor (GDI) activity, inhibiting the rate of exchange of GDP for GTP by $G\alpha_{i1}$. Both regions also stabilize $G\alpha_{i1}$ in its GDP-bound form, inhibiting the increase in intrinsic tryptophan fluorescence stimulated by AlF_4^- . Our results indicate that both RGS12 and RGS14 harbor two distinctly different $G\alpha$ interaction sites: a previously recognized N-terminal RGS box possessing $G\alpha_{i/o}$ GAP activity and a C-terminal GoLoco region exhibiting $G\alpha_i$ GDI activity. The presence of two, independent $G\alpha$ interaction sites suggests that RGS12 and RGS14 participate in a complex coordination of G-protein signaling beyond simple $G\alpha$ GAP activity.

receptor and inhibiting its release of GDP (*i.e.* $G\beta\gamma$ dimers exhibit “guanine nucleotide dissociation inhibitor” (GDI) activity; Refs. 3–5). Upon agonist binding, the GPCR becomes a guanine nucleotide exchange factor (GEF) and promotes replacement of bound GDP for GTP on the $G\alpha$ subunit. The binding of GTP changes the conformation of three “switch” regions within $G\alpha$, allowing $G\beta\gamma$ dissociation. GTP-bound $G\alpha$ and free $G\beta\gamma$ subunits both initiate signals by interactions with downstream effector proteins until the intrinsic guanosine triphosphatase (GTPase) activity of $G\alpha$ returns the protein to the GDP-bound state. Reassociation of $G\beta\gamma$ with GDP-bound $G\alpha$ obscures critical effector contact sites and terminates all effector interactions (6, 7). Hence, the duration of heterotrimeric G-protein signaling is controlled by the guanine nucleotide state of the $G\alpha$ subunit.

We and others have identified a family of GTPase-activating proteins (GAPs) for $G\alpha$ subunits, the “regulators of G-protein signaling” or RGS proteins (8–11). These proteins all contain a hallmark “RGS box,” which accelerates the intrinsic GTPase rate of $G\alpha$ subunits by binding avidly to the transition state for GTP hydrolysis (12). Discovery of RGS box-mediated GAP activity finally resolved the paradox that GPCR-stimulated signals terminate much faster *in vivo* than predicted from the slow GTP hydrolysis rates exhibited by purified $G\alpha$ subunits *in vitro* (13). However, RGS proteins are clearly more than just $G\alpha$ GAPs (14, 15). For example, additional functional domains outside the RGS box have been identified that extend the roles of specific RGS proteins into assembly of novel $G\beta\gamma$ heterodimers (16, 17), cross-talk between heterotrimeric and Ras superfamily G-proteins (18, 19), and coordination between heterotrimeric G-protein and tyrosine-kinase signaling pathways (20).

In 1997, we identified two RGS box-containing proteins, RGS12 and RGS14 (21). Recent, independent analyses of the primary amino acid sequences of RGS12 and RGS14 have led us (22) and Ponting (23) to predict the existence of a novel $G\alpha$ -subunit interaction module within both RGS and non-RGS proteins, the GoLoco motif. Lanier and colleagues (24) independently identified this polypeptide sequence as the “G-protein-regulatory” or GPR motif within AGS3, a protein first isolated in a yeast-based screen for receptor-independent “activators of G-protein signaling.” We have speculated that the GoLoco/GPR motif may possess receptor-independent GEF activity (22), based on the report of Luo and Denker (25) demonstrating *in vitro* guanine nucleotide exchange activity by the GoLoco motif-containing Purkinje-cell protein 2 (Pcp2). We and others have since shown that the four GoLoco motifs of AGS3 possess GDI activity on $G\alpha_i$ subunits (26, 27). In this report, we describe results from yeast two-hybrid and biophysical analy-

In the standard model of heterotrimeric G-protein signaling, cell surface receptors (GPCRs)¹ are coupled to a membrane-associated heterotrimer composed of $G\alpha$, $G\beta$, and $G\gamma$ subunits (1, 2). $G\beta$ and $G\gamma$ form an obligate heterodimer that binds tightly to GDP-bound $G\alpha$ subunits, enhancing $G\alpha$ coupling to

This is an open access article under the [CC BY](https://creativecommons.org/licenses/by/4.0/) license.

* This work was supported by National Institutes of Health Grants GM62338 (to D. P. S.), CA58689, and DK17780 (to M. G. F.).

[‡] Supported in part by NIDDK, National Institutes of Health (NIH), Grant DK07386 and NIGMS, NIH, Grant GM07040.

^{||} A Year 2000 Scholar of the EJLB Foundation and recipient of a Burroughs Wellcome Fund New Investigator Award in the Basic Pharmacological Sciences. To whom all correspondence should be addressed: Dept. of Pharmacology, CB#7365, UNC-Chapel Hill School of Medicine, Mary Ellen Jones Bldg., Rm. 1106, Chapel Hill, NC 27599-7365. Tel.: 919-843-9363; Fax: 919-966-5640; E-mail: dsiderov@med.unc.edu.

¹ The abbreviations used are: GPCR, G-protein-coupled receptor; AGS3Con, AGS3 GoLoco motif consensus peptide; GAP, GTPase-activating protein; GDI, guanine nucleotide dissociation inhibitor; GEF, guanine nucleotide exchange factor; GoLoco, $G\alpha_{i/o}$ -Loco interaction; GTPase, guanosine triphosphatase; R12GL, RGS12 GoLoco motif peptide; R12Scr, RGS12 GoLoco motif scrambled peptide; R14GL, RGS14 GoLoco motif peptide; RBD, Ras-binding domain; RGS, regulator of G-protein signaling; GTP γ S, guanosine 5'-O-(3-thiotriphosphate); PCR, polymerase chain reaction; aa, amino acid(s); SPR, surface plasmon resonance; GST, glutathione S-transferase; RU, response units.

ses designed to address whether the single GoLoco motifs within RGS12 and RGS14 are capable of interacting with $G\alpha$ subunits and affecting their guanine nucleotide cycle.

EXPERIMENTAL PROCEDURES

Materials—BODIPY FL-GTP γ S was purchased from Molecular Probes, Inc. (Eugene, OR). Peptides corresponding to the GoLoco region of rat RGS14 ("R14GL"; ⁴⁹⁶DIEGLVELLNVRVQSSGAHDQRGLLRK-EDLVLPFLQ⁵³¹), a scrambled version of the minimal rat RGS12 GoLoco motif ("R12Scr"; AQLRFISAEAREDNFSFKDEQ), and the consensus sequence (28) from the four GoLoco motifs of AGS3 ("AGS3Con"; TMGEEDFFDLLAKSQSKRMDDQVRVLDAG) were synthesized using conventional Fmoc (*N*-(9-fluorenyl)methoxycarbonyl) blocking group chemistry by the University of North Carolina Peptide Chemistry Group (Chapel Hill, NC). A peptide corresponding to the GoLoco region of rat RGS12 (¹¹⁸⁶EAEFFELISKAQSNRADDQRGLLRKEDLVLP-EFLR¹²²¹) was purchased from New England Peptide Inc. (Fitchburg, MA). All peptides were synthesized with free amine N termini and amide-blocked C termini; peptide purity was confirmed by mass spectrometry and amino acid analyses.

Yeast Two-hybrid Analysis—A panel of $G\alpha$ subunit baits constructed as Gal4p-DNA binding domain fusions in the vector pGBT9 has previously been described (26). A cDNA fragment encoding amino acids 1093–1259 of rat RGS12 was amplified from the full-length rat *Rgs12* cDNA (21) by PCR (sense primer, 5'-CGAATTCTAAGTCTGGATGGACAGCGGGTC-3'; antisense primer, 5'-TCTCGAGTTAGCTCTCTCTGTCTGAAGTCTC-3'), trapped in the pCR2.1-Topo vector (Invitrogen), sequence-verified, and subcloned in frame downstream of the Gal4p activation domain using the *Eco*RI and *Xho*I sites of pACT2. In a similar fashion, a cDNA fragment encoding amino acids 496–544 of rat RGS14 was PCR-amplified from the full-length rat *Rgs14* cDNA (sense primer, 5'-CGAATTCCTGACATTGAAGGCCCTAGTGGAG-3'; antisense primer, 5'-GGTCGACGGGAGGGGCAACAACAG-3') and subcloned into the same sites of pACT2. Bait and prey plasmid pairs were cotransformed into yeast strain SFY526 (CLONTECH), and interactions were analyzed by a qualitative colony lift assay for β -galactosidase expression using 5-bromo-4-chloro-3-indolyl β -D-galactoside (29).

Preparation of Recombinant $G\alpha$ Proteins—Myristoylated, recombinant rat $G\alpha_{13}$ protein was purchased from Calbiochem. His₆-tagged mouse $G\alpha_{o1}$, expressed and purified from a pET15b-based *Escherichia coli* expression vector, was provided as a kind gift from Drs. Laurie Betts and John Sondek (University of North Carolina). The open reading frame of human $G\alpha_{i1}$ was amplified by PCR (sense primer, 5'-ACCATGGGCTGCAGCTGAGCGCCGAGGAC-3'; antisense primer, 5'-AGCGCCGCACTGCAAAAACCTAAAAGAGAC-3') from MarathonTM human brain cDNA (CLONTECH), digested with *Nco*I and *Not*I, subcloned into the *Nco*I/*Not*I sites of pProEX-HTb (Life Technologies, Inc.), sequence-verified, and transformed into *E. coli* strain BL21(DE3). Expression of His₆- $G\alpha_{i1}$ protein was induced with 1 mM isopropyl- β -D-thiogalactopyranoside for 4 h at 37 °C in 1-liter bacterial cultures at an A_{600} of 0.9. Bacterial pellets were frozen at -80 °C, thawed on ice, and resuspended in lysis buffer (100 mM NaCl, 10 mM imidazole, 10 mM Na₂HPO₄, 10 mM NaH₂PO₄, pH 7.5). Cell suspensions were lysed using an AMINCO French press (SLM Instruments Inc., Urbana, IL) and clarified by centrifugation at 100,000 $\times g$ for 25 min. Supernatant was then loaded onto a nickel-nitrilotriacetic acid resin FPLC column (His-Trap; Amersham Pharmacia Biotech), and His₆- $G\alpha_{i1}$ protein was eluted using a gradient of 10 mM to 1 M imidazole in lysis buffer. Eluted protein was cleaved with tobacco etch virus protease (Life Technologies) overnight at 4 °C to remove the His₆ tag, diluted into low salt buffer (25 mM NaCl, 20 mM Tris-HCl, pH 8.0), and loaded onto a 6-ml Source 15Q column (Amersham Pharmacia Biotech). $G\alpha_{i1}$ protein was eluted with an 80-ml gradient of 25–400 mM NaCl, and peak fractions were pooled and resolved using a calibrated 150-ml size exclusion column (Sephacryl S200; Amersham Pharmacia Biotech). Protein was buffer-exchanged into storage buffer (200 mM NaCl, 1 mM MgCl₂, 10 μ M GDP, 1 mM dithiothreitol, 20 mM Tris, pH 7.5, 5% glycerol) and concentrated in a Centriprep Centrifugal Filter Device, YM-30 (Millipore Corp.). The concentrations of all proteins purified in this study were determined by A_{280} measurements upon denaturation in guanidine hydrochloride, and calculation of concentration was based on predicted extinction coefficients.

Preparation of Recombinant GST Fusion Proteins—To create the expression plasmid pGEX4T1-rRGS14H₆, the full-length open reading frame of rat *Rgs14* cDNA (aa 1–544; Ref. 21) was amplified by PCR with primers designed to add a 5'-end *Eco*RV site and a 3'-end His₆ tag/stop codon/*Not*I site (sense primer, 5'-CGATATCGATGCCAGGGAAGC-

CCAAGCAC-3'; antisense primer, 5'-TGCGGCCGCTAGTGATGATG-TGTGGTGTGGTGGAGCCCTCTGAGA-3'), subcloned into the *Sma*I and *Not*I sites of pGEX4T1 (Amersham Pharmacia Biotech). pGEX4T1-rRGS14 Δ GoLoco, encoding a C-terminally truncated open reading frame (aa 1–450) lacking the GoLoco region, was created by introducing a stop codon at codon 451 within pGEX4T1-rRGS14H₆ using the QuikChange site-directed mutagenesis system (Stratagene). pGEX4T2-rRGS14^{496–531}, encoding amino acids 496–531 of rat RGS14 spanning the GoLoco motif, was amplified by PCR (sense primer, 5'-CGAATTCCTGACATTGAAGGCCCTAGTGGAG-3'; antisense primer, 5'-GGTCGACTACTGCAGAAATTCTGGAAGGAC-3') and subcloned into the *Eco*RI and *Sal*I sites of pGEX4T2. pGEX4T3-rRGS14 Δ RGS, encoding amino acids 263–544 of rat RGS14, was PCR-amplified (sense primer, 5'-CGAATTCCTCCGCGAGTCTGGACCTG-3'; antisense primer, 5'-GGTCGACTATGGTGGAGCCTCTGAGAACCTG-3') and subcloned into the *Eco*RI and *Xho*I sites of pGEX4T3. pGEX4T2-rRGS12_{1093–1259} was created by cloning the *Eco*RI/*Xho*I fragment (encoding amino acids 1093–1259) of pACT2-rRGS12GoLoco into the *Eco*RI and *Sal*I sites of pGEX4T2. pGEX4T2-rRGS12_{1093–1228} and pGEX4T2-rRGS12_{1184–1228} plasmids were created based on pGEX4T2-rRGS12_{1093–1259} by sequential rounds of site-directed mutagenesis to introduce a stop codon at codon 1229 and delete codons 1093–1183 (QuikChange system; Stratagene). All expression plasmids were sequence-verified prior to transformation into *E. coli* strain BL21(DE3). Bacteria were grown to an A_{600} of 0.6–0.8 at 37 °C before induction with 1 mM isopropyl- β -D-thiogalactopyranoside. After an additional 4 h at 37 °C, cell pellets were lysed, and GST-fusion protein was purified by glutathione-Sepharose chromatography as previously described (30). GST-RGS14^{496–531} and GST-RGS12_{1184–1228} proteins were further purified by size exclusion chromatography over Sephacryl S200 resin prior to use in biosensor kinetics and GTP γ S binding assays.

Surface Plasmon Resonance (SPR) Biosensor Measurements—SPR binding assays were performed at 25 °C on a BIAcore 2000 (BIAcore, Piscataway, NJ) at the University of North Carolina Macromolecular Interactions Facility. Carboxymethylated dextran (CM5) sensor chips with covalently bound anti-GST antibody surfaces were created as previously described (26). Recombinant GST or GST fusion proteins were bound to separate flow cells of anti-GST surfaces to a density of ~1000 response units (RU), except for the kinetic analyses in which GST-RGS14^{496–531} and GST-RGS12_{1184–1228} were bound to a density of 50 RU. To test the GoLoco interaction with myristoylated $G\alpha_{13}$, GST, GST-RGS14 Δ RGS, and GST-RGS12_{1093–1259} proteins were directly coupled to the carboxymethylated dextran biosensor surfaces (to levels of 5700, 7100, and 6200 RU, respectively) using *N*-hydroxysuccinimide and *N*-ethyl-*N'*-(dimethylaminopropyl)carbodiimide according to the manufacturer's instructions (BIAcore).

As recommended by Lenzen and colleagues (31), binding analyses were performed using Buffer W (150 mM NaCl, 5 mM MgCl₂, 0.005% Nonidet P-40, 20 mM HEPES, pH 7.4) as the running buffer to stabilize the anti-GST antibody surface. Recombinant $G\alpha$ subunits were initially diluted to 1 μ M in Buffer W containing either 32 μ M GDP, 32 μ M GDP plus 32 μ M AlCl₃ and 10 mM NaF, or 32 μ M GTP γ S, incubated for 90 min at 30 °C (or overnight at room temperature for GTP γ S loading of $G\alpha_{i1}$ and myristoylated $G\alpha_{13}$), and further diluted in the same Buffer W plus nucleotide combination prior to injection. 25 μ l of $G\alpha$ protein aliquots were injected at a flow rate of 5 μ l/min over four flow cell surfaces simultaneously using the KINJECT command; for kinetic analyses, injections using the COINJECT command were employed to add a 1.5-fold molar excess of R14GL peptide to the running buffer during dissociation phases. Surface regeneration was performed by serial injections of 5 μ l of 10 mM glycine, pH 2.2, and 5 μ l of 0.05% SDS at a 20 μ l/min flow rate. Background binding to a GST-coated surface (as acquired simultaneously with GST-GoLoco surface binding curves) was subtracted from all binding curves using BIAevaluation software version 3.0 (BIAcore) and plotted using GraphPad Prism version 3.0 (GraphPad Software Inc., San Diego, CA).

Fluorescence-based GTP γ S Binding Assay—Measurements of BODIPY fluorescence were performed with a PerkinElmer Life Sciences LS50B spectrometer with excitation at 485 nm and emission at 530 nm (slit widths each at 2.5 nm). BODIPY FL-GTP γ S was diluted to 1 μ M in 10 mM Tris, pH 8.0, 1 mM EDTA, and 10 mM MgCl₂ and equilibrated to 30 °C in 2-ml cuvettes. 100 nM $G\alpha_o$ or $G\alpha_{i1}$ protein was preincubated with 200 nM GST fusion protein or 400 nM GoLoco peptide at 25 °C for 10 min before the addition to the cuvette. Relative fluorescence levels were set to zero at the average fluorescence reading over the first 70 s, and $G\alpha$ /GoLoco mixtures were added at the 100-s mark.

Spectrofluorometric Analysis of $G\alpha$ Activation by AIF₄⁻—Measurements of intrinsic tryptophan fluorescence were performed on the

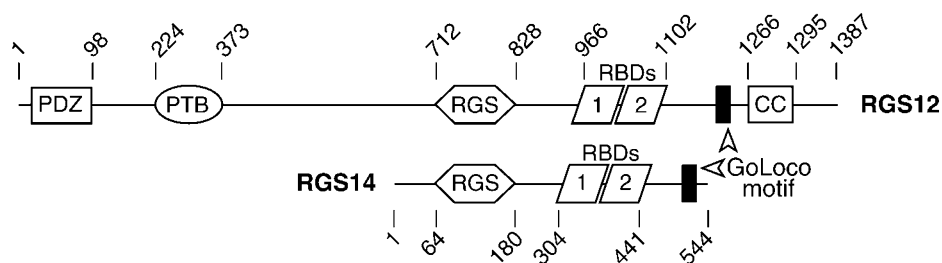


FIG. 1. Schematic illustration of the multidomain composition of rat RGS12 and RGS14 proteins. Numbers above and below the horizontal lines represent amino acid numbering of domain boundaries, corresponding to GenBank™ records U92280 and U92279, respectively. As originally defined (22), the conserved GoLoco motifs (black boxes) are present between amino acids 1188 and 1220 in rat RGS12 and between amino acids 498 and 530 in rat RGS14. CC, coiled-coil region. PTB, phosphotyrosine-binding domain.

LS50B spectrometer with excitation at 292 nm and emission at 342 nm (slit widths 2.5 and 5.0 nm, respectively). Recombinant $G\alpha_o$ and $G\alpha_{i1}$ proteins were diluted in 2-ml cuvettes to 200 nM in preactivation buffer (100 mM NaCl, 100 μ M EDTA, 2 mM $MgCl_2$, 20 μ M GDP, 20 mM Tris-HCl, pH 8.0) and incubated at 30 °C. To activate $G\alpha$, 2 mM NaF and 30 μ M $AlCl_3$ (final concentrations) were added after 400 and 500 s, respectively. To determine the effect of GoLoco-derived peptides on AlF_4^- -induced $G\alpha$ activation, a complex of 400 nM GoLoco peptide and 200 nM $G\alpha$ -GDP was performed in the same buffer and then activated with NaF and $AlCl_3$ additions as described above. Unlike our previous use of the tryptophan-containing GST-AGS3₄₂₄₋₆₅₀ fusion protein (26), the $G\alpha$ fluorescence measurements in this present study were unaffected by peptide fluorescence, since none of the GoLoco peptides tested contains tryptophan residues.

RESULTS

$G\alpha_i$ Subfamily Selectivity by RGS12 and RGS14 GoLoco Regions—The yeast two-hybrid system was used to assess whether the GoLoco motifs of rat RGS12 (aa 1188–1220) and rat RGS14 (aa 498–530) are capable of binding $G\alpha$ subunits. Yeast two-hybrid “prey” were constructed by fusing the Gal4p-activation domain with either a 167-amino acid span of rat RGS12 (aa 1093–1259) or a 49-amino acid span of rat RGS14 (aa 496–544); both regions are C-terminal to the tandem Ras-binding domains (19, 23) and centered about the GoLoco motif (Fig. 1). The yeast reporter strain SFY526 was transformed with pairs of GoLoco-region prey and $G\alpha$ protein “baits” and interactions identified by a qualitative, chromogenic β -galactosidase filter lift assay as previously described (26). Of the $G\alpha$ protein baits tested from all four subfamilies (α_s , α_i , α_q , and α_{12} ; Ref. 32), interaction was only detected between GoLoco-region prey and $G\alpha_{i1}$, $G\alpha_{i2}$, and $G\alpha_{i3}$. In contrast to our previous yeast two-hybrid results with AGS3 (26), no interaction was detected between $G\alpha_o$ and the GoLoco regions of either RGS12 or RGS14 in this assay (Table I).

Guanine Nucleotide-dependent Binding to $G\alpha_i$ Subunits—Although wild-type (and thus presumably GDP-bound) $G\alpha$ subunits were used in the yeast two-hybrid analysis, one possibility is that the observed interactions occurred between GoLoco region prey and a fraction of GTP-bound $G\alpha_i$ bait. Therefore, to assess directly the dependence of GoLoco/ $G\alpha$ interactions on bound nucleotide and also to confirm the observed $G\alpha_i$ binding selectivity, real time binding assays were performed using the SPR technique. RGS12 and RGS14 polypeptides were purified as GST fusion proteins and bound to anti-GST antibody-coated biosensor surfaces at saturating levels. Recombinant $G\alpha_o$ and $G\alpha_{i1}$ proteins were injected for 300 s over these biosensor surfaces, having first been incubated with one of the following guanine nucleotides: GTP γ S (a nonhydrolyzable GTP analog) to mimic the activated GTP-bound form, GDP with AlF_4^- to mimic the transition state of GTP hydrolysis, or GDP alone to preserve the $G\alpha$ subunit in the GDP-bound, inactive state.

Both $G\alpha_o$ and $G\alpha_{i1}$, when preloaded with GDP and AlF_4^- , bound avidly to full-length RGS14 protein (GST-RGS14; Fig. 2A, left panel), as predicted based on the preference of the

TABLE I
Yeast two-hybrid analysis of $G\alpha$ interactions with RGS12 and RGS14 GoLoco motif regions

The β -galactosidase filter-lift assay was performed on Leu- and Trp-deficient media plates, and color intensity was scored after 8 h. –, no color; +, moderate color; ++, strong color; +++, very strong color; ND, not done. Yeast cotransfected with empty bait and prey vectors were assayed for background color development, and none was detected after 20 h of incubation.

Bait ^a	RGS12-GoLoco prey ^b (aa 1093–1259)	RGS14-GoLoco prey ^b (aa 496–544)
$G\alpha_{i1}$	++	+++
$G\alpha_{i2}$	+	+
$G\alpha_{i3}$	+++	+++
$G\alpha_o$	–	–
$G\alpha_z$	–	–
$G\alpha_q$	–	–
$G\alpha_s$	–	–
$G\alpha_{12}$	–	–
$G\alpha_{13}$	ND	–

^a $G\alpha$ baits constructed as Gal4p-DNA binding domain fusions in vector pGBT9 as described in Ref. 26.

^b GoLoco region prey constructed as Gal4p-activation domain fusions in vector pACT2.

RGS14 RGS box to exhibit GAP activity toward $G\alpha_{i/o}$ subunits (19, 33). In addition, avid binding of full-length RGS14 to GDP-bound $G\alpha_{i1}$, but not GDP-bound $G\alpha_o$, was seen. Neither $G\alpha$ subunit bound appreciably to full-length RGS14 when in the activated, GTP γ S-bound form (data not shown).

Deletion of the C-terminal 94 amino acids of RGS14 (aa 451–544), including the GoLoco motif, eliminated binding by GDP-bound $G\alpha_{i1}$ but did not abrogate binding to $G\alpha_o$ -GDP/ AlF_4^- and $G\alpha_{i1}$ -GDP/ AlF_4^- subunits (GST-RGS14 Δ GoLoco; Fig. 2A, middle panel). Conversely, a GST fusion biosensor surface composed solely of the GoLoco motif region of RGS14 (aa 496–531) only interacted with GDP-bound $G\alpha_{i1}$ (GST-RGS14₄₉₆₋₅₃₁; Fig. 2A, right panel).

Avid binding of GDP-bound $G\alpha_{i1}$ was also observed with a GST fusion protein containing a 136-amino acid span of RGS12 (aa 1093–1228) that includes the GoLoco motif (Fig. 2B, left panel). Deletion of amino acids 1093–1183, residues that are N-terminal to the GoLoco motif, did not inhibit $G\alpha_{i1}$ -GDP binding (GST-RGS12₁₁₈₄₋₁₂₂₈; Fig. 2B, right panel). In contrast with results using RGS14, much reduced but still significant binding was also observed between the AlF_4^- form of $G\alpha_{i1}$ and both forms of the RGS12 GoLoco region. To confirm this difference between RGS12 and RGS14 GoLoco regions, recombinant myristoylated $G\alpha_{i3}$ was injected over highly saturated, directly conjugated surfaces of GST-RGS12₁₀₉₃₋₁₂₅₉ or GST-RGS14 Δ RGS proteins. While appreciable binding to GST-RGS14 Δ RGS was only seen upon injection of GDP-bound myristoylated $G\alpha_{i3}$, and not the GDP/ AlF_4^- - or GTP γ S-bound forms (Fig. 2C, left panel), all three forms of myristoylated $G\alpha_{i3}$ bound to some detectable degree to the GST-RGS12₁₀₉₃₋₁₂₅₉ surface. The rank order of binding avidity to GST-RGS12₁₀₉₃₋₁₂₅₉ was

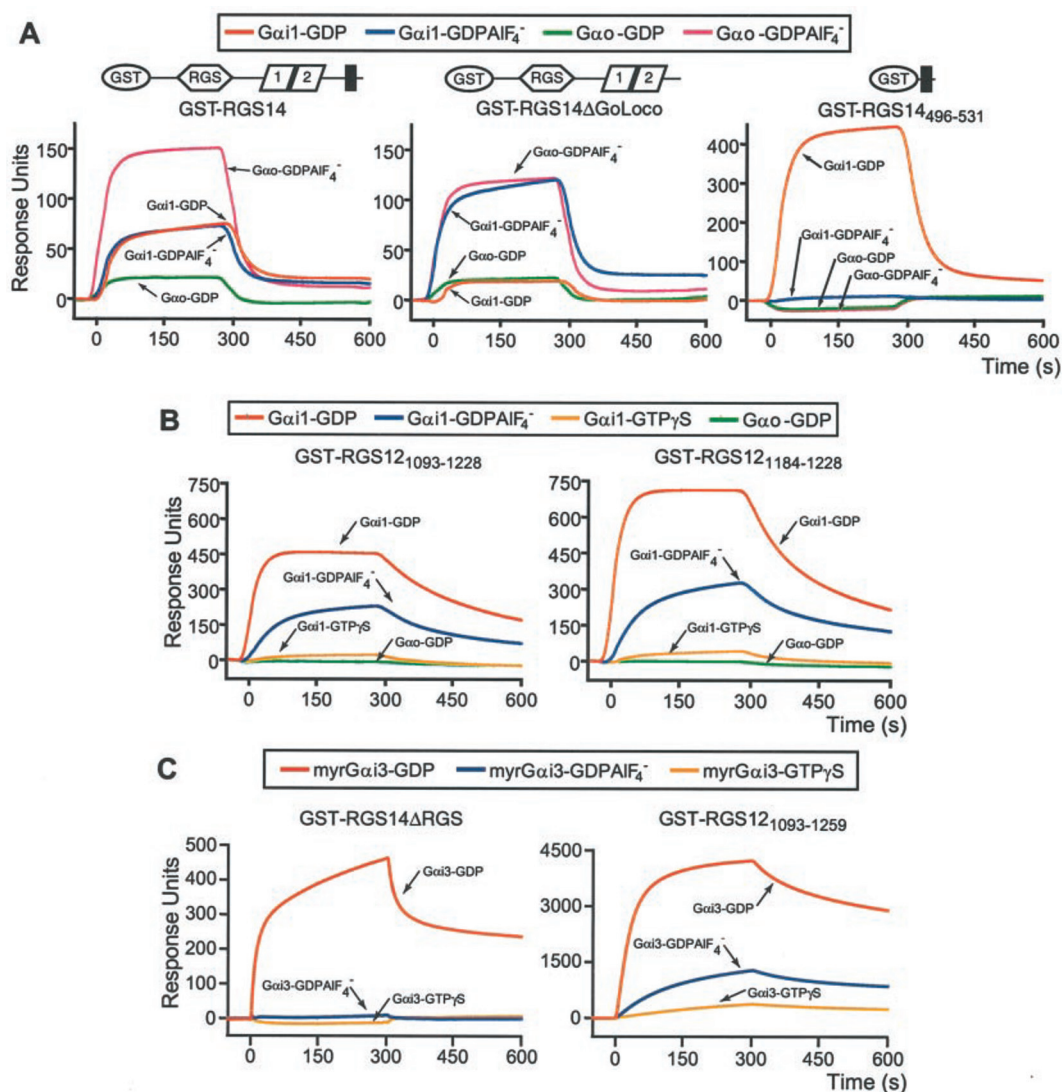


FIG. 2. Guanine nucleotide-dependent binding of $G\alpha_{i1}$ and $G\alpha_{i3}$ to the GoLoco regions of GST-RGS12/14 fusion proteins as assessed by surface plasmon resonance. *A*, responses of anti-GST antibody-coated biosensor surfaces, preloaded to saturation with GST-RGS14 full-length protein (*left panel*), GST-RGS14 Δ GoLoco protein (*middle panel*), or GST-RGS14_{496–531} protein (*right panel*), upon 25- μ l injection (time, 0 s; flow rate, 5 μ l/min) of 100 nM recombinant $G\alpha_{i1}$ or $G\alpha_o$ subunits prebound with GDP or GDP with aluminum tetrafluoride ($GDPAlF_4^-$). Neither $G\alpha$ subunit bound appreciably to any RGS14-derived biosensor surface when in the activated, GTP γ S-bound form (data not shown). *B*, responses of anti-GST biosensor surfaces preloaded to saturation with GST fusion proteins encoding a 136-amino acid (aa 1093–1228; *left panel*) or a 45-amino acid (aa 1184–1228; *right panel*) region of rat RGS12 encompassing the GoLoco motif. $G\alpha$ injections were performed as in *A*. *C*, responses of biosensor surfaces covalently coupled to GST-RGS14 Δ RGS (aa 263–544; *left panel*) or GST-RGS12_{1093–1259} (*right panel*) proteins. 1 μ M of recombinant, myristoylated $G\alpha_{i3}$ prebound with GDP, GDP/ AlF_4^- , or GTP γ S was injected as in *A*. All $G\alpha$ interaction curves displayed are subtracted from response curves generated simultaneously by a separate GST control surface.

clearly $G\alpha_{i3}$ -GDP \gg $G\alpha_{i3}$ -GDP/ AlF_4^- \gg $G\alpha_{i3}$ -GTP γ S (Fig. 2C, *right panel*).

Table II summarizes quantitative kinetic measurements of $G\alpha_{i1}$ -GDP binding to the minimal GoLoco regions of RGS12 and RGS14. Separate, low density (50 RU) biosensor surfaces of either GST-RGS14_{496–531} or GST-RGS12_{1184–1228} protein were prepared, and various concentrations of GDP-bound $G\alpha_{i1}$ (25–4000 nM) were injected over each surface for 300 s. To eliminate biosensor rebinding events during the dissociation of bound $G\alpha$ (*i.e.* during the 300–600-s time interval), a synthetic peptide encompassing the RGS14 GoLoco region (“R14GL”; see below) was injected immediately after the $G\alpha$ association phase; R14GL peptide was injected at a concentration 1.5-fold greater than the preceding $G\alpha_{i1}$ injection (*e.g.* 6 μ M R14GL injection after 4 μ M $G\alpha_{i1}$ -GDP injection). The resultant association and dissociation curves were fit to a Langmuir 1:1 interaction model using BIAevaluation 3.0 software. The resultant kinetically derived dissociation constants (K_D) were 19 nM for

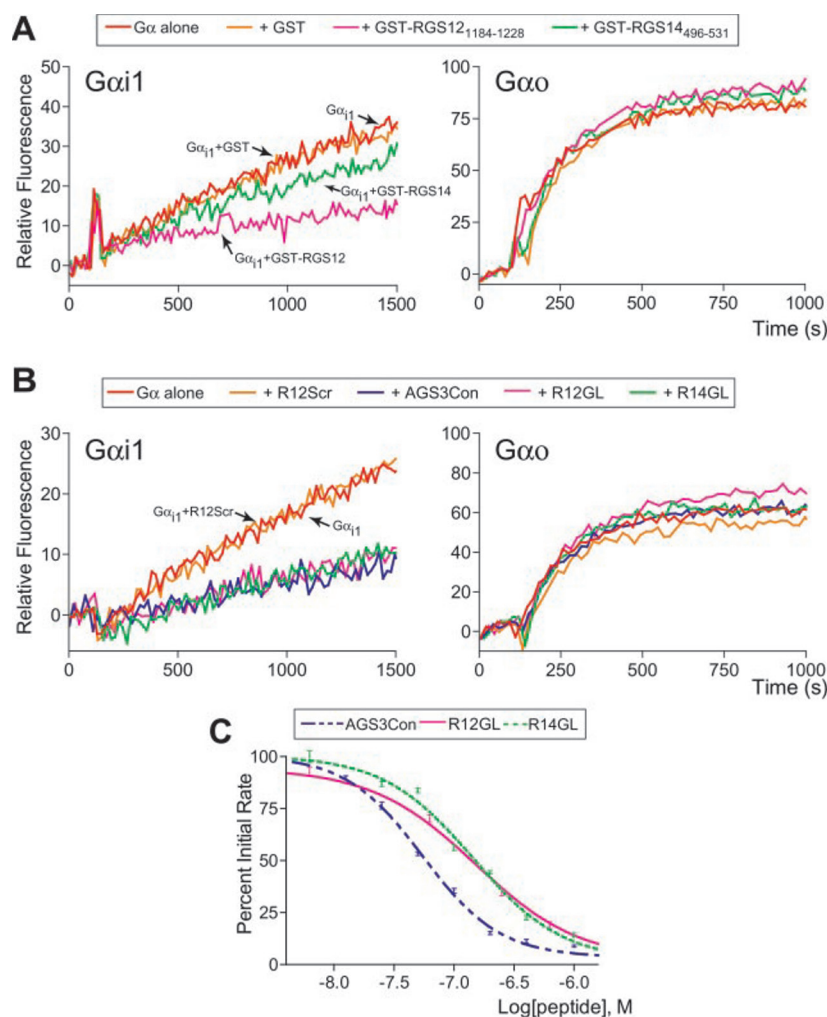
TABLE II
Kinetic parameters for $G\alpha_{i1}$ -GDP interaction with RGS12/14 GoLoco regions as measured by SPR biosensor assays

Biosensor surface	k_a $M^{-1} s^{-1}$	k_d s^{-1}	K_D nM	χ^2
GST-RGS12 _{1184–1228}	$2.89 (4) \times 10^4$	$5.5 (6) \times 10^{-4}$	19	17.5
GST-RGS14 _{496–531}	$2.49 (4) \times 10^3$	$1.6 (4) \times 10^{-4}$	65	3.7

GST-RGS12_{1184–1228} and 65 nM for GST-RGS14_{496–531} (Table II).

GDI Activity of RGS12 and RGS14 GoLoco Peptides—To determine the effect of the RGS12/14 GoLoco region on the guanine nucleotide cycling properties of $G\alpha_i$, we performed a fluorescence-based, real time GTP γ S binding assay. BODIPY FL-GTP γ S is a fluorescent derivative of the commonly used, nonhydrolyzable GTP analog GTP γ S that allows robust real time measurements of GTP γ S binding to $G\alpha$ subunits (34); fluorescence from the BODIPY group is normally quenched by

FIG. 3. GDI activity of RGS12/14 GST fusion proteins and GoLoco-derived peptides on $G\alpha_{i1}$ as measured by fluorescent GTP γ S binding. A and B, time course of BODIPY-GTP γ S binding to 100 nM $G\alpha_{i1}$ -GDP (left panel) and 100 nM $G\alpha_o$ -GDP (right panel) in the absence or presence of 200 nM GST or 200 nM GST-RGS12/14 GoLoco region fusion proteins (A) or 400 nM synthetic peptides (R12GL, R14GL, AGS3Con) derived from the GoLoco regions of RGS12, RGS14, and AGS3, respectively (B). The peptide R12Scr represents a scrambled version of the RGS12 GoLoco polypeptide sequence and clearly exhibits no GDI activity. C, by measuring the initial rates of BODIPY-GTP γ S binding after preincubating 100 nM $G\alpha_{i1}$ -GDP with various concentrations (4 μ M to 0.1 nM) of GoLoco peptides, submicromolar IC_{50} values have been observed for R12GL (151 nM), R14GL (144 nM), and AGS3Con (55 nM).



the guanine base when the nucleotide is in solution, whereas binding to $G\alpha$ abolishes this self-quenching. Preincubation of 100 nM $G\alpha_{i1}$ -GDP with 200 nM GST-RGS14₄₉₆₋₅₃₁ or 200 nM GST-RGS12₁₁₈₄₋₁₂₂₈ prior to the addition of BODIPY FL-GTP γ S reduced the observed initial rate of GTP γ S binding to ~70 and ~30%, respectively, of the initial rate observed for $G\alpha_{i1}$ -GDP alone or $G\alpha_{i1}$ -GDP preincubated with 200 nM GST (Fig. 3A, left panel). This reduction in BODIPY FL-GTP γ S binding, indicative of GDI activity, was also observed upon preincubating $G\alpha_{i1}$ -GDP with one of three GoLoco-derived peptides: 36-amino acid peptides from RGS12 (“R12GL”; aa 1186–1221) or RGS14 (“R14GL”; aa 496–531) or, as a positive control, a 28-amino acid peptide representing the consensus AGS3 GoLoco region sequence (“AGS3Con”; Ref. 28) (Fig. 3B, left panel). No reduction in BODIPY FL-GTP γ S binding was measured after preincubation with a sequence-scrambled version of the RGS12 GoLoco motif (“R12Scr”; Fig. 3B, left panel). In addition, no reduction in BODIPY FL-GTP γ S binding was observed using $G\alpha_o$ (Fig. 3, A and B, right panels), consistent with the lack of RGS12 and RGS14 GoLoco binding to $G\alpha_o$ observed in yeast two-hybrid and biosensor binding assays, as well as our previous report on the lack of AGS3 GDI activity toward $G\alpha_o$ (26).

Quantitation of initial rates of BODIPY FL-GTP γ S binding, after preincubating 100 nM $G\alpha_{i1}$ -GDP with various concentrations (0.1 nM to 4 μ M) of GoLoco peptides, revealed submicromolar IC_{50} values for all three peptides: 151 ± 75 nM (95% confidence interval) for R12GL, 144 ± 40 nM for R14GL, and 55 ± 11 nM for AGS3Con (Fig. 3C). Our results with the AGS3

consensus peptide are consistent with the report by Peterson and colleagues (28) of a ~200 nM IC_{50} for AGS3 for inhibition of [³⁵S]GTP γ S binding to $G\alpha_{i1}$. The observed IC_{50} values for R12GL and R14GL peptides are consistent with the apparent $G\alpha_{i1}$ binding affinities of their GST fusion counterparts as determined by biosensor binding assays detailed above.

GoLoco Peptide Stabilization of Inactive $G\alpha_{i1}$ —The intensity of tryptophan fluorescence by the GDP-bound forms of $G\alpha_i$ subunits increases significantly upon activation by AlF_4^- ; this enhanced intrinsic fluorescence is considered a hallmark of the activated state (35, 36). We previously reported that binding of the tetra-GoLoco C terminus of AGS3 to $G\alpha_{i3}$ -GDP significantly inhibits activation by AlF_4^- as measured by real time spectrofluorometry of intrinsic $G\alpha_{i3}$ tryptophan fluorescence (26). The ability of GoLoco-derived peptides to inhibit AlF_4^- activation of $G\alpha_{i1}$ and $G\alpha_o$ was tested using the same system.

While preincubation of GDP-bound $G\alpha_{i1}$ with peptide R12Scr had no effect on AlF_4^- activation kinetics, preincubation with a 2-fold molar excess of peptides R12GL, R14GL, or AGS3Con significantly inhibited $G\alpha_{i1}$ activation (Fig. 4A). The fluorescence of GoLoco peptide-bound $G\alpha_{i1}$ did not attain the level of AlF_4^- -activated $G\alpha_{i1}$, even upon extended incubation (30 min; data not shown). None of the GoLoco-derived peptides had any discernible effect on the AlF_4^- activation kinetics of $G\alpha_o$ (Fig. 4B), again consistent with the binding and functional assays presented here for RGS12 and RGS14 and previously for AGS3 (26). These results suggest that the GoLoco peptides derived from RGS12, RGS14, and AGS3 inhibit the conformational change in $G\alpha_i$ subunits necessary to accommodate AlF_4^- and

FIG. 4. **GoLoco-derived peptides selectively stabilize $G\alpha_{i1}$ in its inactive GDP-bound form.** Activation of 200 nM $G\alpha_{i1}$ (left panel) and 200 nM $G\alpha_o$ (right panel) by AlF_4^- is measured by the enhancement of intrinsic tryptophan fluorescence. $G\alpha$ subunits were preincubated either alone or with the indicated GoLoco-derived peptide in a 2-fold molar excess. 20 mM NaF was added at 400 s, and 20 μ M $AlCl_3$ was added at 500 s. Tryptophan fluorescence was monitored by spectrofluorometry as described under "Experimental Procedures."

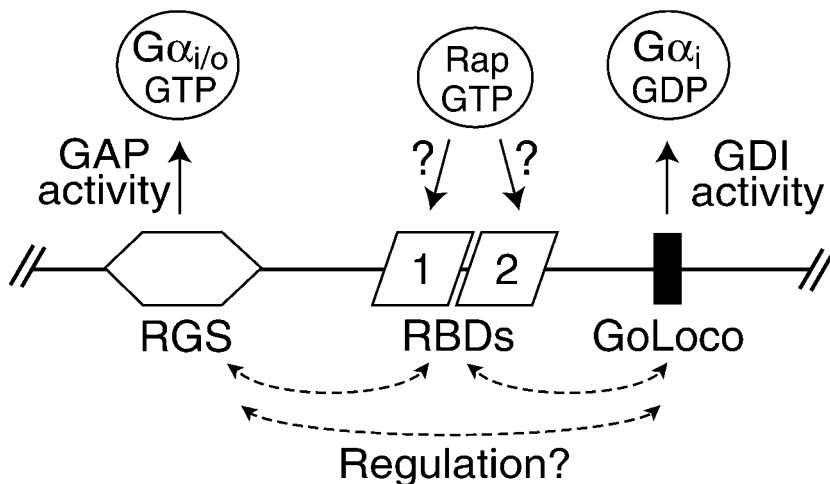
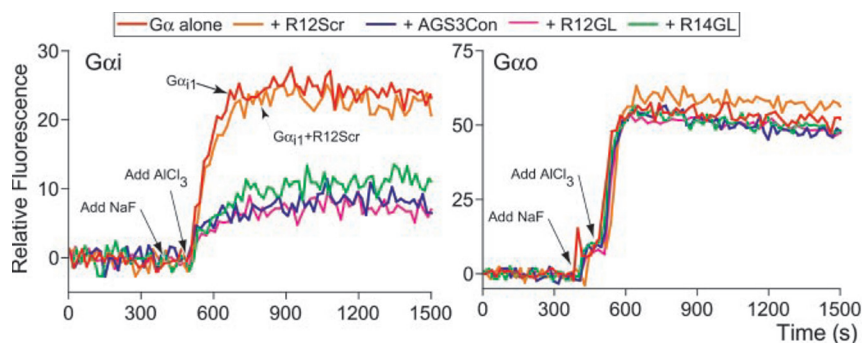


FIG. 5. **Schematic illustration of the potential functional interplay between the RGS box, RBD domains, and GoLoco region found within both RGS12 and RGS14.** Documented biochemical activities on heterotrimeric $G\alpha$ subunits or Ras superfamily GTPases are denoted with *solid arrows* above the respective regions. Potential modes of regulation of these biochemical activities are marked with *dashed arrows* below the respective regions.

thus stabilize $G\alpha_i$ in the inactive, GDP-bound state.

DISCUSSION

Since our original identification of RGS12 and RGS14 (21), several functional domains beyond the defining RGS box have been recognized within both proteins. We discovered an N-terminal PDZ (PSD-95/Dlg/ZO-1) domain within the largest RGS12 isoforms and described its exquisite binding specificity for C-terminal (A/S)TX(L/V) motifs (30). We also identified an N-terminal phosphotyrosine-binding domain (14) and have recently described its involvement in recruiting RGS12 to the N-type calcium channel via neurotransmitter-stimulated tyrosine kinase activity (20). By bioinformatic analyses, Ponting (23) identified putative Ras-binding domains (RBDs) within both RGS12 and RGS14; Traver and colleagues (19) subsequently illustrated that this region in RGS14 interacts with GTP-bound Rap1 and Rap2. These findings have led to the realization that RGS12 and RGS14 are not simply $G\alpha$ GAPs but are rather multifaceted signal transduction regulators (14, 15).

We previously predicted a second $G\alpha$ -interaction site, distinct from the RGS box, within the C termini of RGS12 and RGS14 (22). Our prediction was based on *in silico* identification of the GoLoco motif within both proteins and other known $G\alpha$ interactors including AGS3, Pcp2, and LOCO, the *Drosophila* homolog of RGS12 and RGS14. We also speculated that the GoLoco motifs of RGS12 and RGS14 may activate $G\alpha$ -GDP subunits via GEF activity (14), based on a demonstration of $G\alpha_o$ -directed GEF activity *in vitro* by recombinant Pcp2, a GoLoco-containing protein (25). We confirm our prediction in this present study but not our speculation. We have shown that both RGS12 and RGS14 indeed contain a second $G\alpha$ interaction site centered about the GoLoco motif; this site binds avidly and specifically to GDP-bound $G\alpha_i$ subunits. However, we also found that $G\alpha_{i1}$ -GDP binding to RGS12/14 GoLoco regions *in-*

hibits both GTP γ S binding and AlF_4^- -induced activation. These results suggest that, rather than enhancing nucleotide release, these GoLoco regions act as GDIs and impede $G\alpha_i$ activation.

The binding and biochemical activities of the RGS12/14 GoLoco regions appear specific for $G\alpha_i$ subunits, and no analogous activity was observed toward $G\alpha_o$. This selectivity is consistent with reports that the GDI activity of AGS3 is specific for $G\alpha_i$ subunits, although an AGS3/ $G\alpha_o$ interaction is seen in yeast two-hybrid assays (26–28). The structural basis underlying selective binding and regulation of GDP-bound $G\alpha_i$ subunits by RGS12, RGS14, and AGS3 GoLoco regions is currently unknown. $G\alpha_{i1}$, $G\alpha_{i2}$, and $G\alpha_{i3}$ are clearly more closely related to each other (93–97% pairwise similarity) than to $G\alpha_o$ (81–82% pairwise similarity). Since conformational changes within $G\alpha$ switch regions are central to the structural differences between GDP- and GTP-bound states (37), one explanation for selective GoLoco binding to $G\alpha$ -GDP would be direct interaction of GoLoco motif residues with $G\alpha$ switch region(s). It is interesting to note, therefore, that several amino acid differences exist between $G\alpha_o$ and $G\alpha_{i1-3}$ in the otherwise highly conserved switch regions II and III (*i.e.* Asp²¹⁸, Gln²³³, His²³⁶, Thr²⁴⁰, and Thr²⁴¹ of mouse $G\alpha_i$; Ref. 38). These switch region differences could explain the profound selectivity of RGS12/14 GoLoco regions for $G\alpha_i$ and not $G\alpha_o$. We are currently pursuing experimentally derived atomic resolution structural data on the GoLoco/ $G\alpha_i$ interface to confirm the relative importance of the switch regions to $G\alpha$ binding selectivity. Such structural data should also clarify whether GoLoco-mediated inhibition of AlF_4^- activation arises from frank blockade of the AlF_4^- binding pocket or inhibition of the resultant structural changes that occur in $G\alpha$ upon AlF_4^- docking. Given the surface plasmon resonance binding results of Fig. 2, it is unlikely that the GoLoco motifs of RGS12 and RGS14 are capable of displacing AlF_4^- bound to the G-protein.

The $G\alpha_i$ subunit selectivity of the RGS12/14 GoLoco regions is not shared with the N-terminal RGS boxes. Not only have we shown here that both $G\alpha_{i1}$ and $G\alpha_o$ bind avidly to the RGS14 RGS box upon AlF_4^- activation (Fig. 2), but we and others have previously observed GAP activity by RGS12 and RGS14 RGS boxes on both $G\alpha_{i1}$ and $G\alpha_o$ subunits in single-turnover assays (19, 30, 33). It is important to note that neither the RGS boxes nor the GoLoco regions interact with $G\alpha_{12}$ or $G\alpha_{13}$ subunits (Table I, Refs. 30 and 33).² Therefore, neither $G\alpha$ interaction site within RGS12 and RGS14 directly explains the recent reports of attenuated signaling by $G\alpha_{12}$ and $G\alpha_{13}$ upon cellular overexpression of RGS12 or RGS14 (33, 39).

The presence of two, independent $G\alpha$ interaction sites (this work) as well as tandemly arrayed Ras-binding domains (19, 23) within both RGS12 and RGS14 suggests that both proteins engage in regulatory cross-talk between heterotrimeric G-protein signaling pathways and Ras superfamily, "small" G-protein signaling pathways. What is currently unclear, however, is the functional interplay between these domains (Fig. 5). Does occupancy of one G-protein interaction site affect the function of the other(s)? For example, does the binding of $G\alpha_i$ -GDP to the GoLoco region affect the capacity of the tandem RBDs to bind Ras family members and/or the capacity of the RGS box to exhibit $G\alpha_{i/o}$ GAP activity? Conversely, does binding of either $G\alpha$ -GTP to the RGS box or Rap-GTP to the RBD(s) modulate the GDI activity of the GoLoco domain? While Traver and colleagues (19) have proposed that RGS14 represents a novel effector for Rap based on selective association with the GTP-bound form of this Ras-related GTPase, there is currently no evidence that the function of the RGS box or the GoLoco region is modulated by Rap-GTP/RBD interaction. Now that binding partners and *in vitro* biochemical activities are assigned to these functional domains, the next challenge will be to define their intramolecular cross-regulation within RGS12 and RGS14 as well as their net result in modulating cellular signaling networks.

Acknowledgments—We thank Dr. Richard R. Neubig (University of Michigan, Ann Arbor) for sharing protocols regarding use of BODIPY-GTP γ S prior to publication, Dr. John E. Sondek for access to the LS50B spectrometer, Dr. T. Kendall Harden for unwavering support and critical review of the manuscript, Michelle Pliske for help with protein purification, and Jennifer Hillman for technical assistance.

REFERENCES

- Gilman, A. G. (1987) *Annu. Rev. Biochem.* **56**, 615–649
- Hamm, H. E. (1998) *J. Biol. Chem.* **273**, 669–672
- Brandt, D. R., and Ross, E. M. (1985) *J. Biol. Chem.* **260**, 266–272
- Higashijima, T., Ferguson, K. M., Sternweis, P. C., Smigel, M. D., and Gilman, A. G. (1987) *J. Biol. Chem.* **262**, 762–766
- Clapham, D. E., and Neer, E. J. (1997) *Annu. Rev. Pharmacol. Toxicol.* **37**, 167–203
- Ford, C. E., Skiba, N. P., Bae, H., Daaka, Y., Reuveny, E., Shekter, L. R., Rosal, R., Weng, G., Yang, C. S., Iyengar, R., Miller, R. J., Jan, L. Y., Lefkowitz, R. J., and Hamm, H. E. (1998) *Science* **280**, 1271–1274
- Li, Y., Sternweis, P. M., Charnecki, S., Smith, T. F., Gilman, A. G., Neer, E. J., and Kozasa, T. (1998) *J. Biol. Chem.* **273**, 16265–16272
- De Vries, L., Mousli, M., Wurmser, A., and Farquhar, M. G. (1995) *Proc. Natl. Acad. Sci. U. S. A.* **92**, 11916–11920
- Siderovski, D. P., Hessel, A., Chung, S., Mak, T. W., and Tyers, M. (1996) *Curr. Biol.* **6**, 211–212
- Berman, D. M., Wilkie, T. M., and Gilman, A. G. (1996) *Cell* **86**, 445–452
- Dohlman, H. G., and Thorner, J. (1997) *J. Biol. Chem.* **272**, 3871–3874
- Tesmer, J. J., Berman, D. M., Gilman, A. G., and Sprang, S. R. (1997) *Cell* **89**, 251–261
- Arshavsky, V. Y., and Pugh, E. N., Jr. (1998) *Neuron* **20**, 11–14
- Siderovski, D. P., Strockbine, B., and Behe, C. I. (1999) *Crit. Rev. Biochem. Mol. Biol.* **34**, 215–251
- De Vries, L., Zheng, B., Fischer, T., Elenko, E., and Farquhar, M. G. (2000) *Annu. Rev. Pharmacol. Toxicol.* **40**, 235–271
- Snow, B. E., Krumins, A. M., Brothers, G. M., Lee, S.-F., Wall, M. A., Chung, S., Mangion, J., Arya, S., Gilman, A. G., and Siderovski, D. P. (1998) *Proc. Natl. Acad. Sci. U. S. A.* **95**, 13307–13312
- Sondek, J., and Siderovski, D. P. (2001) *Biochem. Pharmacol.* **61**, 1329–1337
- Hart, M. J., Jiang, X., Kozasa, T., Roscoe, W., Singer, W. D., Gilman, A. G., Sternweis, P. C., and Bollag, G. (1998) *Science* **280**, 2112–2114
- Traver, S., Bidot, C., Spassky, N., Baltauss, T., De Tand, M. F., Thomas, J. L., Zalc, B., Janoueix-Lerosey, I., and Gunzburg, J. D. (2000) *Biochem. J.* **350**, 19–29
- Schiff, M. L., Siderovski, D. P., Jordan, J. D., Brothers, G., Snow, B., De Vries, L., Ortiz, D. F., and Diversé-Pierluissi, M. (2000) *Nature* **408**, 723–727
- Snow, B. E., Antonio, L., Suggs, S., Gutstein, H. B., and Siderovski, D. P. (1997) *Biochem. Biophys. Res. Commun.* **233**, 770–777
- Siderovski, D. P., Diversé-Pierluissi, M. A., and De Vries, L. (1999) *Trends Biochem. Sci.* **24**, 340–341
- Ponting, C. P. (1999) *J. Mol. Med.* **77**, 695–698
- Takesono, A., Cismowski, M. J., Ribas, C., Bernard, M., Chung, P., Hazard, S., III, Duzic, E., and Lanier, S. M. (1999) *J. Biol. Chem.* **274**, 33202–33205
- Luo, Y., and Denker, B. M. (1999) *J. Biol. Chem.* **274**, 10685–10688
- De Vries, L., Fischer, T., Tronchère, H., Brothers, G. M., Strockbine, B., Siderovski, D. P., and Farquhar, M. G. (2000) *Proc. Natl. Acad. Sci. U. S. A.* **97**, 14364–14369
- Natochin, M., Lester, B., Peterson, Y. K., Bernard, M. L., Lanier, S. M., and Artemyev, N. O. (2000) *J. Biol. Chem.* **275**, 40981–40985
- Peterson, Y. K., Bernard, M. L., Ma, H., Hazard, S., III, Graber, S. G., and Lanier, S. M. (2000) *J. Biol. Chem.* **275**, 33193–33196
- Guarente, L. (1983) *Methods Enzymol.* **101**, 181–191
- Snow, B. E., Hall, R. A., Krumins, A. M., Brothers, G. M., Bouchard, D., Brothers, C. A., Chung, S., Mangion, J., Gilman, A. G., Lefkowitz, R. J., and Siderovski, D. P. (1998) *J. Biol. Chem.* **273**, 17749–17755
- Lenzen, C., Cool, R. H., Prinz, H., Kuhlmann, J., and Wittinghofer, A. (1998) *Biochemistry* **37**, 7420–7430
- Simon, M. I., Strathmann, M. P., and Gautam, N. (1991) *Science* **252**, 802–808
- Cho, H., Kozasa, T., Takekoshi, K., De Gunzburg, J., and Kehrl, J. H. (2000) *Mol. Pharmacol.* **58**, 569–576
- McEwen, D. P., Gee, K. R., Kang, H. C., and Neubig, R. R. (2001) *Anal. Biochem.* **291**, 109–117
- Higashijima, T., Ferguson, K. M., Sternweis, P. C., Ross, E. M., Smigel, M. D., and Gilman, A. G. (1987) *J. Biol. Chem.* **262**, 752–756
- Phillips, W. J., and Cerione, R. A. (1988) *J. Biol. Chem.* **263**, 15498–15505
- Lambright, D. G., Noel, J. P., Hamm, H. E., and Sigler, P. B. (1994) *Nature* **369**, 621–628
- Wall, M. A., Posner, B. A., and Sprang, S. R. (1998) *Structure* **6**, 1169–1183
- Mao, J., Yuan, H., Xie, W., Simon, M. I., and Wu, D. (1998) *J. Biol. Chem.* **273**, 27118–27123

² A. M. Krumins, D. P. Siderovski, and A. G. Gilman, unpublished data.